# Nuclear Morphometry, Epigenetic Changes, and Clinical Relevance in Prostate Cancer

Robert W. Veltri and Christhunesa S. Christudass

**Abstract** Nuclear structure alterations in cancer involve global genetic (mutations, amplifications, copy number variations, translocations, etc.) and epigenetic (DNA methylation and histone modifications) events that dramatically and dynamically spatially change chromatin, nuclear body, and chromosome organization. In prostate cancer (CaP) there appears to be early (<50 years) versus late (>60 years) onset clinically significant cancers, and we have yet to clearly understand the hereditary and somatic-based molecular pathways involved. We do know that once cancer is initiated, dedifferentiation of the prostate gland occurs with significant changes in nuclear structure driven by numerous genetic and epigenetic processes. This review focuses upon the nuclear architecture and epigenetic dynamics with potential translational clinically relevant applications to CaP. Further, the review correlates changes in the cancer-driven epigenetic process at the molecular level and correlates these alterations to nuclear morphological quantitative measurements. Finally, we address how we can best utilize this knowledge to improve the efficacy of personalized treatment of cancer.

**Keywords** Prostate cancer • Epigenetics • Nuclear morphology • Nuclear roundness

## Abbreviations

AR      Androgen receptor
CaP     Prostate cancer
CT      Chromosome territory

R.W. Veltri, Ph.D. (✉) • C.S. Christudass
The Brady Urological Research Institute, Park 213, Johns Hopkins Hospital,
600 N Wolfe Street, Baltimore, MD 21287, USA
e-mail: rveltri1@jhmi.edu; cchris38@jhmi.edu

CCD       Charge coupled device
HGPIN     High-grade prostate intraepithelial neoplasia
IHC       Immunohistochemistry
NE        Nuclear envelope
NET       Nuclear envelope transmembrane protein
NMD       Nuclear morphometric descriptor
NRF       Nuclear roundness factor
NRV       Nuclear roundness variance
PRC2      Polycomb repressive complex 2
PSA       Prostate-specific antigen
QNG       Quantitative nuclear grade
RP        Radical prostatectomy
TSA       Trichostatin A

## Introduction

Rudolf Virchow [1] published his famous aphorism "omnis cellula e cellula" ("every cell stems from another cell"), and he launched the field of cellular pathology and stated that all diseases involve changes in normal cells, that is, all pathology ultimately is cellular pathology. Further, for over 140 years it has been shown that nuclear morphology is often disrupted in cancer. In the 1860s, Lionel S. Beale [2, 3] of King's College Hospital examined unstained sputum from a patient with cancer of the pharynx and observed nuclear morphology variations in the cancerous cells. Lionel Beale also established a private laboratory near the King's College Hospital and gave a course of lectures on "The Microscope in Medicine" which included practical demonstrations in clinical pathology. He also wrote books on infectious disease theory and the practical value of the microscope in medicine to exam urine, blood, tumor tissue, and infectious agents. Subsequently, with many advances in microscopy, cytologic and anatomic pathologists recognized the importance of cell as well as nuclear structure in cancer diagnosis and prognosis.

In terms of early advances in cell biology, Theodor Boveri (1862–1915) was the first to use the term "chromosome territory" (CT). Although Boveri was able to observe nuclear dynamics, he was reliant solely on fixed materials and inferior microscopic instrumentation, whereas many decades later the efforts of Cremer et al. [4, 5] gave additional meaning to CT. In Boveri's 1909 publication, he described chromatin movements and organization in three observational hypotheses [6]. First, CT arrangements are stably maintained during interphase. Second, that chromosome stability is lost during prometaphase and there are greater movements of CTs. Finally, the daughter nuclei exhibit symmetry with each other and the general radial CT positioning between mother/daughter nuclei is maintained. Chromatin is organized into specific structural domains, likely by association with distinct nuclear compartments that are enriched in regulatory or nuclear structural proteins such as the nuclear matrix and associated attachment proteins as well as nuclear

envelope transmembrane protein (NET)/lamina proteins, etc. [4, 5, 7]. Importantly, gene activity is modulated by interactions with several of these subnuclear compartments and specific protein elements of the nuclear envelope (NE). The organization of the chromosomes is based on CT positioning and allows late replicating genes and gene-poor chromosomes to be located at the nuclear periphery, while early replicating genes and gene-rich chromosomes are more centrally disposed, suggesting that many inactive genes are located at the periphery of the normal cell nucleus [8]. In spite of our increased understanding of how genomes are organized into CTs and where genes tend to be spatially expressed in normal cells; once cancer is initiated and progresses the chromosomes often become disorganized with either approximately the same amount of chromosomal material observed after the genetic alteration (balanced) or a major loss and/or gain of chromosomal material involved after the alteration (unbalanced) [4, 5, 7].

*The "gold standard" for detection of cancer remains the pathologist's detection of gross changes in cellular (nucleus and cytoplasm) and tissue structure and organization.*

Today, nuclear morphology measures include nuclear size, shape, DNA content (ploidy), and chromatin organization. The microscope and several improvements in the microscope lens, lighting, charge-coupled device (CCD) digital cameras, and novel software for analyzing images over the years have allowed for the detailed observation and study of nuclear size, shape and chromatin texture in cells, which clearly indicated abnormalities in cancer cells [7, 9]. Also, the development of histochemical stains provided significant improvements to study cancer cell and tissue morphology [10]. Hematoxylin was demonstrated to form a dye–metal complex with arginine-rich basic (cationic) nucleoproteins such as histones. Eosin dye is acidic in nature and tends to bind to more eosinophilic cellular structures (cytoplasm, collagen and muscle fibers) producing various shades of pink. Combining hematoxylin and eosin (H and E) enabled study of nuclear structure and its internal organization. George Papanicolaou developed a stain that enables visualization of many cytoplasmic and nuclear structural features of cells in the 1930s, and applied the stain to cervical cells to test for cancer—the so-called "Pap test" [11]. The Pap stain for cytology combines hematoxylin stain for tissues with phosphotungstic acid-Orange G solution and two sulfonic groups ($SO_3Na$) and the eosin with two auxochromic groups (COONa and NaO). The latter are acid dyes that demonstrate an attraction to basic proteins, such as prekeratin. H and E staining is usually performed on paraffin-embedded formalin fixed tissues and is read and interpreted by an anatomic pathologist, while the Pap stained slides are fixed in alcohol preparations and read and interpreted by a cytopathologist.

Also, the Feulgen staining reagent was developed for nuclei because it specifically and quantitatively stoichiometrically binds to DNA. The Feulgen reagent binds to DNA by uncovering the free aldehyde groups in DNA during the acid hydrolysis process, which then reacts with the reagent via a Schiff-Base interaction to form a stable, bluish/purple colored compound that absorbs light at 560 nm [12, 13]. In order to best interpret the Feulgen stained nuclei, a microspectrophotometer microscope fitted with a 3CCD color camera is employed to capture the information

based on equations that calculate nuclear size, shape, texture and DNA content with DNA ploidy based on a single step pixel map of each nucleus [13]. Our laboratory employs the AutoCyte Pathology Workstation (APW, TriPath Inc., Burlington, NC, USA) with QUIC-DNA V1.201 software that is capable of measuring several nuclear morphometric descriptors (NMDs) to calculate a quantitative nuclear grade (QNG) from the NMDs in. An example of the Feulgen stain and an artificially colored 3D single nucleus is shown for a normal, high grade prostate intraepithelial neoplasia (HGPIN) and prostate cancer (CaP). The information collected on about 150 cancer epithelial cells can be used to predict grade, stage, biochemical recurrence, metastasis, and survival for CaP [7, 9].

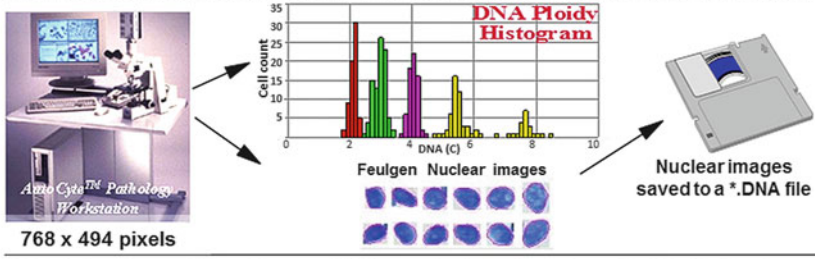## Clinical Translational Relevance of Nuclear Structure in Prostate Cancer

It is imperative to be aware that the Gleason System for CaP histopathological grading is not based at all on nuclear grading; rather it is based on the assessment of dedifferentiation of glandular tissue architecture in CaP area (their altered size, shape, and distribution) when viewed under a low power microscope (final magnification 100–200×) by an expert pathologist. Donald Gleason devised the original scheme that established five patterns (Grade 1–5) to describe well differentiated to moderately and poorly differentiated cancer glands that has held up for the most part [14, 15]. Prognosis is based upon the fact that less aggressive prostate tumors have more of an appearance of normal glandular tissue, whereas more aggressive tumors that are more likely to invade and metastasize differ significantly from normal tissue owing to a loss of benign glandular architecture in terms of their size, shape, and distribution (poorly differentiated), as well as other histological features of tissue architecture including changes in the nuclear chromatin structure seen with H and E staining. To assign a Gleason score, the pathologist first looks for a dominant (primary) pattern of tumor cell growth or grade (the area where the cancer is most prominent) and then looks for a less widespread pattern or grade (secondary), and gives each one a grade number. The Gleason score is the sum of the dominant, or primary, tissue pattern grade (representing the majority of tumor) and the less dominant, or secondary, tissue pattern grade (assigned to the minority of the tumor). Today, pathologists tend to describe a Gleason score of 5 or 6 as a low-grade cancer, 7 (3+4 or 4+3) as medium-grade, and 8, 9, or 10 as high-grade cancer and then interpret a prognosis that includes the Gleason score as well as additional clinical information [16]. Occasionally, a pathologist may note a small area of a higher grade pattern in a biopsy or radical prostatectomy (RP) specimen known as a "tertiary pattern" and may record this result, because it may be prognostically relevant with time [16, 17]. A lower-grade cancer tends to grow more slowly and is less likely to invade and spread than a cancer with a higher grade pattern. Some limitations for the Gleason score system involve interpretations when comparing a biopsy to RP specimens, reproducibility of Gleason grading due to subjective interpretation amongst multiple pathologists and difficulty in diagnosing small acinar atypical

lesions [17]. Our research has been focused on extracting information from the cancer and the benign adjacent nucleus, which can exceed the subjective evaluation of the CaP patient glandular architecture (Gleason grade patterns) as a variable to predict CaP outcomes and be used for intervention decisions [7, 9, 16, 17].

Alternative approaches to assess cancer involve characterization of nuclear structure through several approaches including manual, semi-automated, or automated machine vision techniques to assess architecture from H and E formalin-fixed paraffin-embedded tissue preparations. Diamond et al. [18] utilized a manual Graphpad software with a microscope to trace up to 300 malignant and benign nuclei from each CaP patient. Next, they compared nuclear size and shape in a set of prostate organ-confined CaP cases that had long-term follow-up and determined that they could distinguish those with a good prognosis from those with a poor prognosis (metastasis) with high accuracy ($p < 0.005$). Defining a circle as 1.0, they calculated the nuclear roundness factor (NRF) as follows: $NRF = (C/2\pi)/(A/\pi)1/2$ ($C$ = circumference and $A$ = area), whereas the circularity form factor = $4\pi A/C^2$. The text below illustrates several applications of this technology; however, it has not been commercialized for practical use by pathologists. Dr Donald Coffey's laboratory and Dr. Mitchell Benson compared the use of flow cytometry (where the nuclei were labeled with acridine orange) to measure light scatter (forward and perpendicular) with the nuclear roundness factor performed on the same nuclei to assess tumor aggressiveness and heterogeneity of several well to poorly differentiated rat Dunning prostate tumor cell lines [19, 20]. The correlation between flow cytometry and nuclear roundness factor variance (NRV) using nuclear tracing was exceptional. Later, others using commercially available hardware and software validated the clinical value of NRV measurements using a microscope. The images were analyzed with the DynaCell Motility Morphometry Measurement workstation (JAW Associates, Inc., Annapolis, MD, USA). With this method, measurements varied by less than 5 % among examiners, and the authors confirmed that this NRV shape variable readily predicts progressive disease and mortality of CaP [21–23]. Finally, Veltri et al. [24] showed that the accuracy of NRV assessed by DynaCell technology is significantly higher than the Gleason score to predict metastasis and CaP-specific death in men with long-term follow-up (median follow-up of 17 years). Therefore, nuclear architecture (irregularity of nuclear shape) when accurately quantified is a significant variable to predict aggressive CaP outcomes and NRV exceeds the prognostic value of Gleason grade patterns or score to predict the long-term survival in this patient sample.

Another alternative digital imaging approach described by Veltri et al. [7] used the APW and Feulgen stained prostatic nuclei to study the CaP in biopsy and RP specimens [7, 9]. Our laboratory uses these nuclear images and the ~40 NMDs captured by the APW using DNA QUIC DNA V1.201 software to process the nuclear images and then calculate a QNG illustrated in Fig. 1 determined from the NMDs to make predictions of grade, stage, metastasis, and survival [7, 9]. The technology was also used by Badalament et al. [25] to create a nuclear morphometric QNG signature combined with serum prostate-specific antigen (PSA) to predict stage using ROC analysis with an AUC = 86 % (sensitivity = 85.7 %; specificity = 71.3 %). This was at a time when the staging of CaP based on biopsy informatics was about 50 % accurate. A limitation of this early algorithm was the number of nuclear features
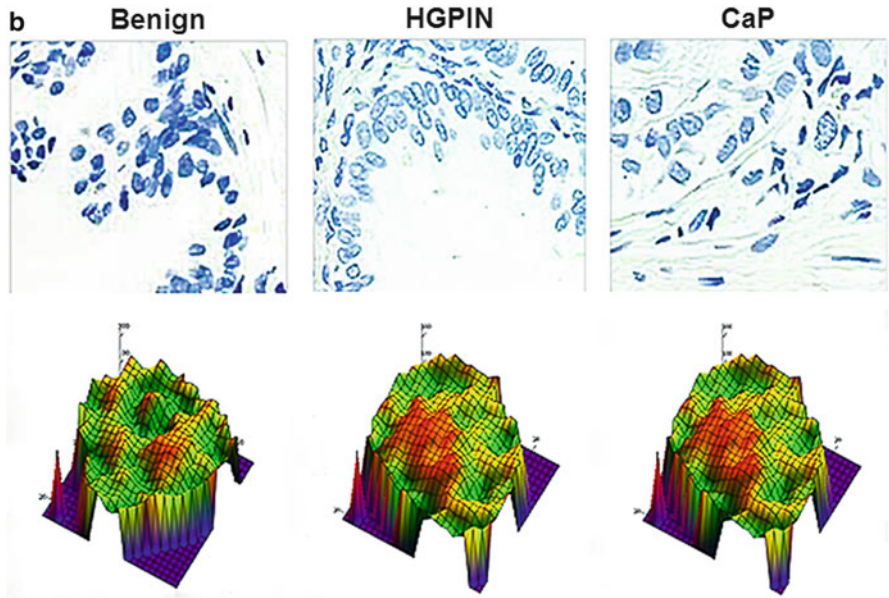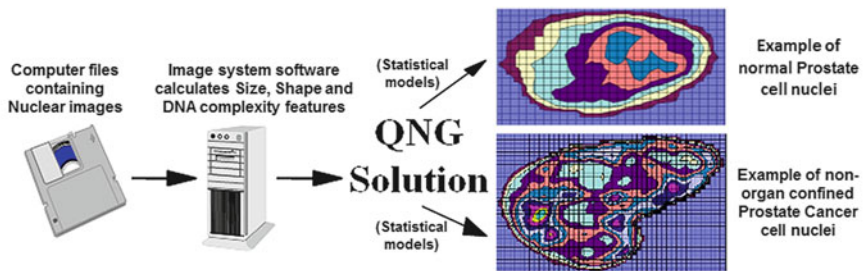
**Fig. 1** Automated analysis of nuclear pathology in prostate cancer (**a**) General Description of the AutoCyte Pathology Workstation's operation. (**b**) Images of single 2D Feulgen stained prostate benign, high grade prostate intraepithelial neoplasia (HGPIN), and prostate cancer nuclei (*left to right*, *upper panels*). These *blue* colored epithelial nuclei are captured by the APW software (QUIV DNA) and 40 nuclear morphometric descriptors (NMDs) are used to calculated image-based solutions for CaP outcomes. In the *bottom panel* is a 3D construction of the nuclear pixel grey level map (made using Mathcad) shows variations in nuclear chromatin labeled with the Feulgen DNA stain

available and the stringency for the Multivariate Logistic Regression (MLR) modeling. However, when the model was applied to incoming biopsy specimens at a urology pathology company, the algorithm performed within 5 % of specifications. Veltri et al. [26] also studied the biopsies of 557 consecutive men that underwent RP at Johns Hopkins Hospital from October 1998 to January 2000. Combining QNG, the Gleason score and complexed PSA density (complete model) yielded a ROC AUC = 82.4 % (sensitivity = 73.5 %; specificity = 83 %) to predict non-organ-confined CaP from a biopsy. Next, Veltri et al. [27] used the APW system and Feulgen stained nuclei to capture 38 nuclear morphometric descriptors to predict CaP biochemical progression. The patient cohort included 115 patients with clinically localized CaP, and the mean follow-up period in 70/115 patients without disease progression was 10.4 ± 1.7 years. Using backward stepwise MLR and the variances of 11/38 of the nuclear morphometric descriptors to calculate QNG were found to be significant for predicting biochemical progression ($p = 0.00001$; ROC AUC = 86 %; sensitivity = 78 %; specificity = 83 %). Furthermore, the QNG and the postoperative Gleason score, when combined, created a MLR model for the prediction of biochemical progression, yielding a ROC AUC = 92 % and having a sensitivity of 89 % and specificity of 84 %. These two parameters (QNG and Gleason score) separated the 115 patients into three statistically significant risk groups based upon Kaplan–Meier plot analysis. Predicting aggressive CaP effectively depends on having a sufficient sample size and long-term follow-up data for the successful application of nuclear morphometry as a variable in addition to routine pathological and clinical variables. In order to assess aggressive CaP using QNG Khan et al. [28] successfully predicted progression to metastasis and/or CaP mortality in 227 RP surgical specimens by employing the APW imaging system and applying the QNG analysis. The combined pathology-QNG model retained lymph node status, prostatectomy Gleason score, and QNG, yielding a ROC AUC = 86 % with an accuracy of 76 % at 90 % sensitivity. Next, Veltri et al. [29] employed the same digital imaging technology and the APW to calculate a QNG solution using a tissue microarray made from 0.6 mm tissue cores of 182 patients (cancer and adjacent benign areas) to evaluate the use of QNG alone and with pathological and clinical variables to predict metastasis and death due to CaP. The pathology model yielded a ROC AUC = 72.5 %. We assessed the QNG solution determined by MLR statistical models for the adjacent benign and cancer areas and yielded a ROC AUC = 81.6 % and 79.9 %, respectively. Hence, semi-automated digital image analysis can use nuclear NMDs to make clinical outcome predictions; however, the technology requires time and expertise to perform reproducibly whether or not it is a manual or semi-automated NRV single variable or a QNG signature methodology. Hence, commercialization continues to be a challenge unless automation can be readily accomplished.

Other applications for quantitative nuclear morphometry based on the APW system permit studies that correlate alterations in nuclear structure with biological and clinical aspects of CaP. Using a NCI Cooperative Prostate Cancer Tissue Resource tissue microarray of 92 cases with long-term follow-up (56 non-recurrences and 36 recurrences), our laboratory [24] demonstrated that the histone acetyltransferase p300 protein (p300, HAT) alters CaP cancer cell nuclear structure and predicts biochemical progression. In this study we also demonstrated that specific nuclear
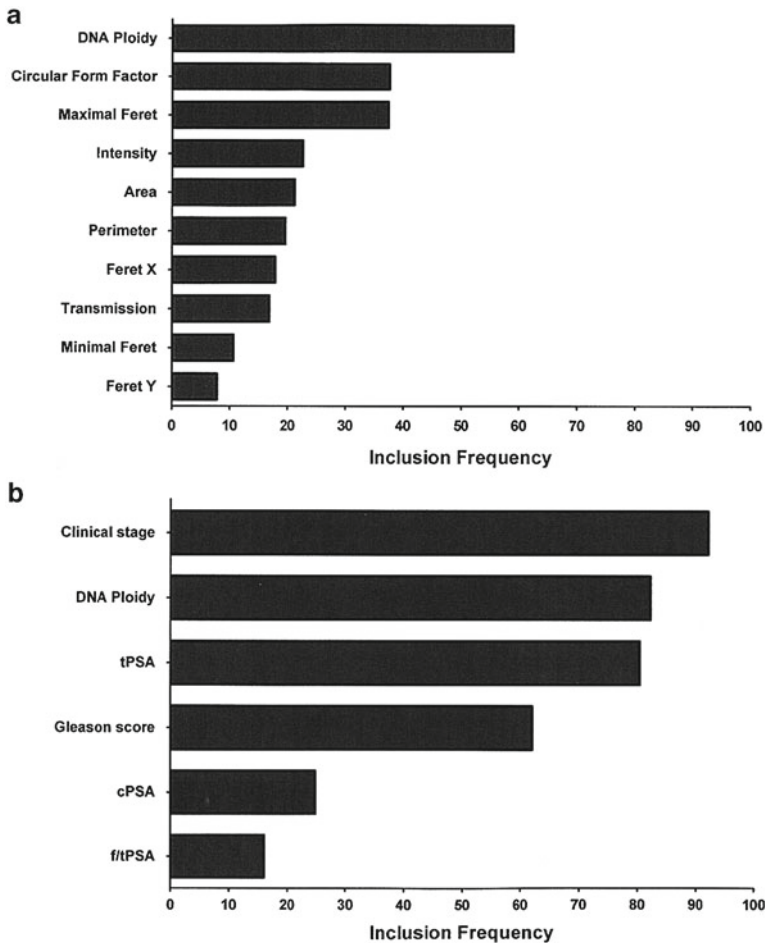
**Fig. 2** Statistical contribution of nuclear morphometry in predicting prostate cancer. Bar graph of the statistical contribution of nuclear morphometry (**a**) and clinical pathological features combined with morphometry (**b**) based on boot strapping (200×) a cox proportional hazards model analysis to predict organ-confined prostate cancer. Notably DNA Ploidy is retained in a multivariate prediction model for organ-confined PCa

features, i.e., circular form factor (rho=−0.26; $p=0.012$) and minimum Feret (rho=−0.21; $p=0.048$) exhibited significant correlations with p300 protein expression. The quantitative immunohistochemistry (qIHC) of the p300 protein expression in high grade tumors (Gleason score ≥ 7) was significantly higher compared to low grade tumors (17.7 % versus 13.7 %, respectively, $p=0.03$). Further, p300 expression remained significant in the Cox multivariate model independent of Gleason score ($p=0.03$). Also, CaP patients with a Gleason score ≥ 7 and p300 IHC expression >24 % showed the highest risk for CaP biochemical recurrence ($p=0.002$) in a Kaplan–Meier plot. Using the same imaging technology we showed

that nuclear features predict non-organ-confined CaP [26]. In Fig. 2a we show the nuclear morphometric features correlate with organ-confined disease status in CaP. Note that DNA ploidy was the most frequently included feature in a MLR bootstrap model and that several nuclear shape factors were also useful. In Fig. 2b using the same MLR method, we compared the contribution of clinical and pathological features to make the same decision and of note is that DNA ploidy was very comparable to clinical stage in this patient cohort ($n = 370$) and when combined in a clinicopathological model discriminates organ confined from non-organ-confined CaP [26]. Another application is the correlation of nuclear morphometry changes to demonstrate the response of CaP cells to histone deacetylase Inhibitors (e.g., Valproic acid; VPA) [30]. In vitro tissue microarrays consisted of CaP cell lines that were treated for 3, 7 or 14 days with 0, 0.6 or 1.2 mM VPA. In vivo the tissue microarrays consisted of cores from CaP xenografts from nude mice treated for 30 days with similar concentrations of VPA achieved in drinking water. Digital images of at least 200 Feulgen stained nuclei were captured and nuclear alterations were measured. Both in vitro and in vivo VPA treatment of CaP cells resulted in significant dose- and time-dependent changes in nuclear structure. Hence, quantitative nuclear morphometry may be useful as a biomarker to assess pathological status of men with CaP, and pave the way for therapeutics based on the proteins or genes that alter chromatin structure and nuclear morphometry [7, 9].

Today, the emergence of the rapid scanning microscope image analysis and the development of novel machine vision imaging techniques is aiding pathologists to analyze histologic tissue images and distinguish cancer grades. Automated image applications have been the recent focus for CaP and other cancers [31, 32]. The development of machine vision techniques has been applied to H and E stained tissue sections, aiding pathologists to analyze CaP tissue images and evaluate the grade patterns of CaP, which has made steady progress during the past decade. As the CaP malignancy is manifested by the loss of the normal glandular architecture (i.e., shape, size, and differentiation of the glands, i.e., Gleason grade patterns) [16, 17], applications of image analysis to improve segmentation and texture analysis to assess different Gleason grading patterns based on H and E and Feulgen stained tissue images have been reported [7, 13, 33, 34]. Numerous machine vision approaches to nuclear size, shape and texture analysis of these images have been applied. Wavelet and multiwavelet transforms, fractal analysis, texton forest/random tree, and cell network cycles have been utilized for texture feature extraction and classification in studies of the automated Gleason grading [33–43]. Collaborating with Dr. Anant Madabhushi at Case Western Reserve University, we codeveloped an image computational method to assess nuclei in Gleason graded CaP. Dr. Madabhushi applied a novel adaptive active contour scheme (AdACM) machine vision method that combines nuclear segmentation boundary and a solid geometry graphic term that includes shape etc. (Fig. 3) [35]. The technique reduces the computational time required in half (250 s for 120 nuclei), measured in seconds; the approach uses the nuclear shape "prior term" in the variational formula and is only invoked for those instances in the image where nuclear overlaps between objects are identified. By not having to invoke all three nuclear feature terms (shape, boundary, and region) for segmenting every nuclear object in the image, the computational expense of the

## Adaptive Active Contour Model (AdACM) to separate Gleason Grade pattern 3 from 4
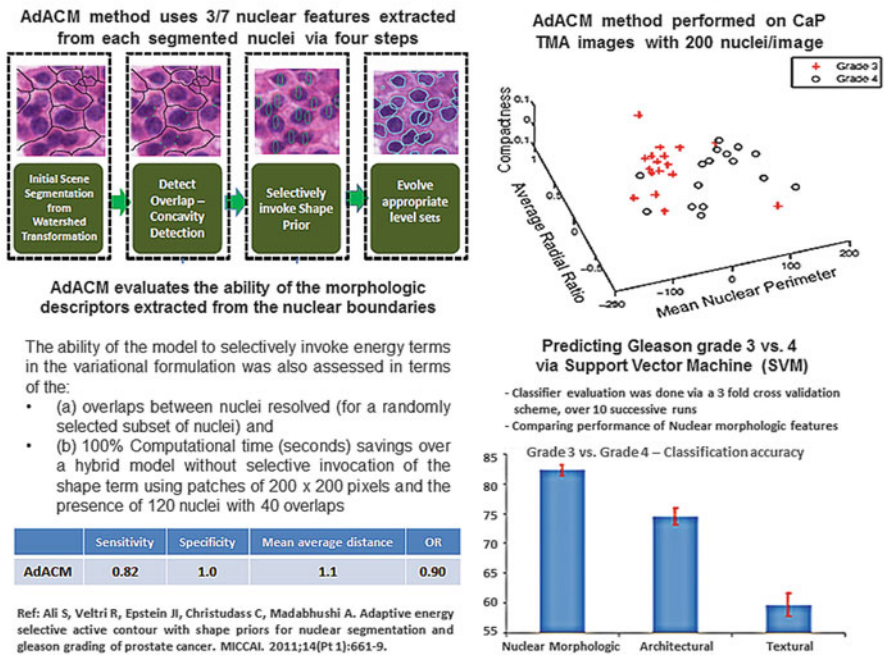


**Fig. 3** This figure demonstrates how AdACM computer-assisted image analysis can separate Gleason grade pattern 3 from 4. The graph in the *upper right* panel shows how three features can accurately separate 3 from 4 (Odds Ratio=0.90). In the *top left hand* panel of the figure, the segmentation method is described. In the *bottom right* panel of the figure, the plot depicts the contribution of nuclear morphology, architecture, and texture to the computational solution plot in the *upper right* hand space

integrated active contour model is dramatically reduced. The AdACM [35] method was employed for the task of segmenting nuclei on CaP tissue microarray core images. Morphological, architectural and textural features extracted from these segmented nuclei were found to able to discriminate different Gleason grade patterns 3 (indolent) and 4 (aggressive) with a ROC AUC=86 % via a mathematically derived classifier and using only three nuclear features. The "nuclear morphologic features" proved to be the best predictor of the three features captured for the study (Fig. 3). Additional collaborative machine vision computational techniques should help to determine if our approaches can predict time-dependent CaP outcomes such as biochemical recurrence, metastasis, and survival.

Using the same CaP tissue microarray in collaboration with Dr. Li with Yoon at the University of Pittsburgh Electrical Engineering department we applied wavelet machine vision technology called cardinal multiridgelet transform (CMRT) [44] to analyze CaP histological H and E images and extract nuclear texture features in the transform domain. CMRT provides cardinality, orthogonally, approximate translation invariance and rotation invariance of the transform. With 48 tissue microarray

images of Gleason grade 3 and grade 4 as a training set and using nuclear texture features extracted there from, a support vector machine with Gaussian kernel was trained to classify grade 3 and grade 4. The leave-one-out cross-validation assessment showed the model accuracy was 93.75 % and a ROC AUC = 0.96 to make this critical pathological separation. Please note this wavelet approach produced similar results to AdACM in terms of time and accuracy. At this point we realize the value of an automated approach to nuclear morphometry in a clinical setting, but yet we do not clearly understand why and how the nuclear shape may be altered in normal differentiation versus cancer dedifferentiation to a malignant state. Hence, in the future we can apply automated computer machine vision technology to process tissue images and extract pathologically relevant prognostic features such as a new cancer grade concept and combine this data with molecular biomarkers.

## Why Does Nuclear Architecture Change in CaP?

Epigenetics involves alterations in gene expression or cellular phenotype that are caused by other mechanisms beyond changes in the DNA sequence through mutations, amplifications, deletions, copy number variations, etc. Examples of epigenetic change include chemical modifications of the histone tails as well as DNA methylation, which over time have often been mired in controversy regarding the heritability of such changes. It is difficult to sort out the concept of heritability in this review. However, we need to accept the premise that environment may be playing an important role in "phenotype plasticity" through transcription of genes that alter cellular and tissue phenotype. Hence, rather than argue this point I have chosen the option to accept the concept in order to address the question of epigenetic events that play key roles in altering the cancer phenotype during initiation and progression [7, 9, 24].

Since the nucleus is a major focus in this review, the anatomy of the NE and its interactions with the key nuclear components of chromatin and DNA will be highlighted. Under normal conditions the NE separates nuclear and cytoplasmic functions and at its inner surface it provides a docking site for chromatin via several NETs and the intermediate filament lamins [45, 46]. The major structural elements of the NE are the inner nuclear membrane, the outer nuclear membrane, the nuclear pore complexes, and the nuclear lamins. Notable, is the importance of alterations in nuclear structure in cancer and the role of the NE and its NETs and associated inner and outer membrane parts [45, 46] (i.e., lumen/perinuclear space [45], ribosomes [45–47], nuclear pores [45, 47–49], nuclear lamina (A, B, and C) [48, 49], nuclear matrix [50, 51], etc.) and their functional interplay during normal cell proliferation, cell differentiation, and carcinogenesis [46]. All of these NE components can impact nuclear architecture (size, shape, and integrity), genome stability (chromosome spatial topology, chromatin regulation, nuclear matrix organization, and gene expression) as well as cell functions (e.g., DNA repair, cell signaling, cell cycle, and mitosis) during carcinogenic progression [45, 46, 52–58]. Additionally, histone modifications such as acetylation, methylation, ubiquitination, and phosphorylation

are extremely critical to regulation of gene transcription and chromatin organization in normal, differentiating stem and cancer cells [57, 59, 60]. Further, critical environmentally driven factors such as occupational or behavioral exposure to carcinogens, diet and metabolism, inflammation and infection, etc., can produce dramatic epigenetic changes that drive alterations in gene activation and suppression causing multiple structural changes in nuclear shape, size and chromatin organization that may generate valuable early diagnostic and prognostic information regarding the pathology and pathogenesis of malignancy [53, 59–63].

One facet of the epigenetic molecular machinery that could drive cancer events involves chromatin remodeling by proteins in the Polycomb group (PcG) and their interaction with nucleosomes (linked by histone H1). Nucleosomes are composed of 140–145 bp of DNA wrapped around the histone octamer that consists of two copies each of H2A, H2B, H3, and H4 (Fig. 4). The enzyme-catalyzed chemical modification of selected amino acids of histones is a mechanism used throughout the living world to increase and regulate the functional plasticity of gene expression. Such molecular plasticity involves several histone modifications at the N-terminal tails that methylate lysine or arginine, acetylate lysine, phosphorylate serine, threonine, or tyrosine, and ubiquitinate lysine, each of which can influence specific gene expression to alter phenotypic changes via modifications to chromatin structure and architecture [54, 57, 59, 60]. Several residues on the tails of histone H3 (e.g., H3K4, H3K9, H3K27, H3K36), as well as in the core of histone H3 (e.g., H3K79) have been shown to be sites for such modifications that are involved in transcriptional regulation and alterations in chromatin organization. Additionally, such histone modification–demodification cycles can directly or indirectly influence DNA methylation. For example, high levels of H3K4 methylation correlates with low levels cytosine methylation at CpG dimers; levels of H3K4 methylation are influenced by other H3 modifications, including acetylation, which can exert an indirect effect on DNA methylation; and methylation of H3 at K9 or K36 can influence levels or positioning of DNA methylation [54, 57, 59, 60]. In mammals DNA methylation occurs at the cytosines of CpG dimers in DNA. The deamination of 5-methyl cytosine (meC) forms thymidine, resulting in a G-T base mismatch, the repair of which could result in the replacement of either base. Replacement of the G with an A results in a mutated DNA sequence, in which the original meC is replaced with T. Hence, epigenetic changes inevitably weave together chemical modifications of histones with DNA methylation events causing phenotypic changes through the influence of environmental agents, which can also produce genetic changes (i.e., mutations, deletions, amplifications, etc.) that promote cancer [54]. Clearly, in cancer, histone modifications lie at the heart of mechanisms by which a variety of functionally significant nuclear proteins activate (oncogenes) or silence specific regions (i.e., tumor suppressor genes) of the human genome. These alterations involve transcription factors, chromatin modifying enzymes, the complexes that methylate DNA, or the chromatin remodelers that reposition nucleosomes along the DNA strand [58, 59, 64]. Recently, in a breast cancer model (MCF-7), Tropberger et al. [63] have functionally characterized acetylation of H3K122 and revealed that H3K122 acetylation
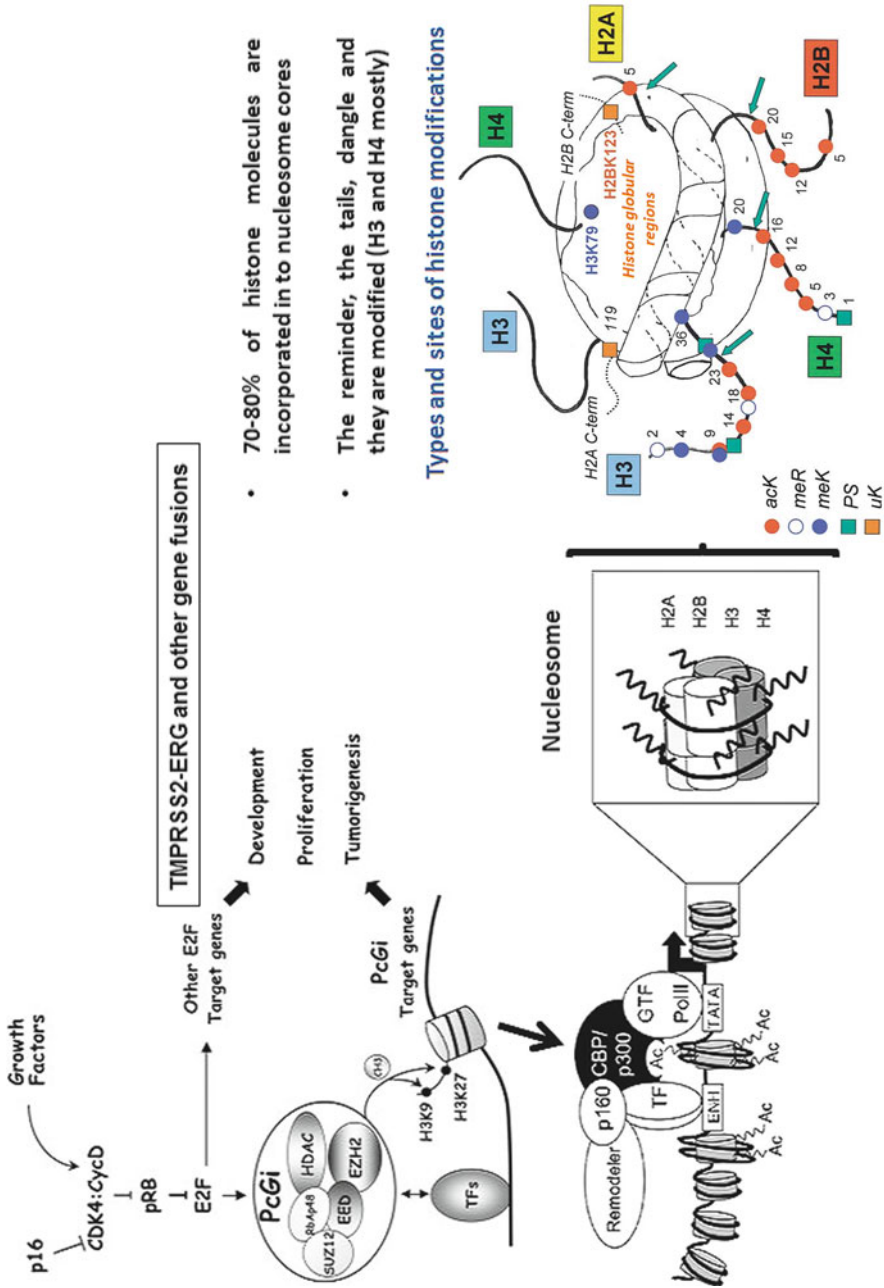
**Fig. 4** Epigenetic marks involved in tumorigenesis. The illustration shows the interaction of Polycomb 2 transcription complex with the nucleosome transcription complex as well as sites for modification of the histones

is catalyzed by p300/CBP and can be sufficient to stimulate transcription in vitro. They showed that H3K122 acetylation is specifically enriched at active transcription start sites and enhancers as well as on H3.3- and H2A.Z-containing nucleosomes. H3K122 is modified by acetylation at estrogen-regulated genes and marks enhancers actively engaged in transcriptional regulation. Finally, the authors showed that mutation of H3K122 can impair transcriptional activation in vivo and have proposed a model for H3K122 acetylation on the lateral nucleosome surface changing chromatin structure to promote transcription in breast tumors.

Aberrant epigenetic events such as DNA hypomethylation and hypermethylation and altered histone acetylation and methylation have been observed in CaP affecting the expression and function of a large array of genes that can lead to tumorigenesis, tumor progression, and metastasis. Initially CaP is androgen dependent, but can eventually become androgen independent after androgen deprivation therapy. Androgen-independent CaP is characterized by a heterogeneous loss of androgen receptor (AR) expression [61, 62, 65, 66]. AR promoter methylation is more prevalent in androgen-independent CaP than in primary androgen-dependent CaP, suggesting that epigenetic silencing of AR by DNA hypermethylation could be an alternative mechanism leading to androgen independence in a subset of advanced CaP patients. Similarly, in CaP the importance of histone modifications and progression has been studied. To be clinically applicable, an ideal prognostic tumor biomarker must be readily detectable in noninvasive clinical specimens. DNA hypermethylation and histone modifications alter nuclear architecture, fulfilling this requirement, and thus are promising biomarkers [67]. Jarrard et al. [68] reported aberrant promoter methylation in AR-negative CaP cell lines. These results are consistent with the results of Izbicka et al. [69] that showed 5,6-dihydro-5-azacytidine, an inhibitor of cytosine DNA methyltransferase, could restore androgen sensitivity in androgen insensitive human CaP cell lines, which then become sensitive to growth inhibition by anti-androgens. Human cancers almost ubiquitously harbor epigenetic alterations. There is strong evidence that some epigenetic alterations (e.g., DNA hypermethylation and hypomethylation) are heritable and can also be dynamically altered during CaP progression. Recent research has demonstrated using "cityscape plots" a wide range of epigenetic plasticity and support that DNA methylation alterations have the potential for producing selectable driver events in CaP carcinogenesis and disease progression [67].

In the area of histone modifications and their application to CaP prognosis, Seligson et al. [70] conducted IHC on a tissue microarray of 226 CaP cases of which 183/226 (81 %) showed changes in IHC expression for histones: acetylated (Ac) H3K9, H3K18, H4K12, and dimethylated (diMe) H4R3 and H3K4. The objective was to predict biochemical recurrence, defined as a postoperative serum PSA of 0.2 ng/ml or greater and was seen in 61 (34 %) of all study patients, and 20 (19 %) of patients with low grade tumors. The median follow-up time within the recurring and non-recurring patient groups was 22.0 (range 1.0–115.0) and 65.5 months (range 2.0–163.0). In a multivariate Cox Proportional Hazards Ratio model the histone modification panel had a value of 3.86 (95 % CI=1.18–12.62), $p$=0.025. The two groups are identified on the basis of the "simple clustering rule" involving only

H3K18Ac and H3K4diMe modifications. The study also included a validation set of 39 cases with low grade CaP that were analyzed according to the above simple rule involving H3K18Ac and H3K4diMe and the IHC staining distinguishes between two groups of patients with risks of tumor recurrence: 4 % in group A versus 31 % in group B (log-rank $p = 0.016$; hazard ratio = 9.2; 95 % CI 1.02–82.2). Recent studies by Bianco-Miotto et al. [71] on global patterns of specific histone modifications revealed an epigenetic signature for CaP involving H3K18Ac and H3K4diMe. The authors studied histone modifications in 279 cases of CaP and they showed that H3K18Ac and H3K4diMe when combined are predictors of relapse-free survival, with high global levels associated with a 1.71-fold ($p < 0.0001$) and 1.80-fold ($p = 0.006$) increased risk of tumor recurrence, respectively. These high levels of both histone modifications were associated with a threefold increased risk of relapse ($p < 0.0001$). Further, the study revealed an epigenetic gene expression candidate gene signature for CaP that included several interesting epigenetic genes (DNMT3A, MBD4, MLL2, MLL3, NSD1, and SRCAP), which significantly discriminated non-malignant from CaP tumor tissue ($p = 0.0063$). Notably, of those six genes altered between primary and metastatic CaP, DNMT3A, MLL2, NSD1, and MLL3 were significantly downregulated and MBD4 and SRCAP upregulated tumor in the primary prostate cancer samples with biochemical recurrence when compared with the primary samples without recurrence. In the metastatic samples, these same genes were also significantly altered, with DNMT3A, MLL2, NSD1, MBD4, and MLL3 upregulated and SRCAP downregulated when compared with the primary prostate tumors. The prognostic classification on the validation set therefore confirmed the predictive power of histone modifications as markers of CaP prognosis.

In another study Watson et al. [72] used digital texture analysis to assess global chromatin patterns following treatment of normal (PNT1A) and CaP (LNCaP) cell lines with trichostatin-A (TSA) and observed significant alterations in the TSA induced H3K9 hyperacetylation resulting in decondensation of heterochromatin, which was associated with altered gene expression profiles in both the immortalized normal PNT1A prostate cell line and a malignant androgen-dependent CaP cell line LNCaP. Though some changes were TSA dose dependent and cell cycle dependent, flow cytometric analysis enabled the observation of clear differences in chromatin decondensation and H3K9 acetylation between the normal and tumor lines.

Our laboratory studied the protein expression profiling of the Dunning rat CaP cell lines of varying metastatic potential [G (0 %), AT-1 (>20 %), and MLL (100 %)] using SELDI-TOF-MS [73]. We identified a 17.5 km/z SELDI-TOF-MS peak that was found to retain discriminatory value in each of two separate study sets that was verified as histone H2B. The increases in the histone H2B peak correlate with the metastatic potential of the Dunning cell lines, going up slightly in the AT-1 subline and consistently increasing more strongly in the MLL subline. Clearly, the above results obtained to date support that signatures of global histone modifications and histone levels are associated with prognostic features of CaP. Also, other publications demonstrate that alterations in the expression of histone remodeling enzymes may represent novel diagnostic and prognostic markers of CaP and potentially new targets for therapeutics [74, 75]. Therefore, global epigenetic modifications in androgen

sensitive and resistant CaP can activate or repress multiple genes that impact nuclear chromatin architecture as well as CaP progression to metastasis [61, 65–75].

PcG, which is best known for its role in silencing the HOX gene cluster during embryonic development [76, 77], acts by forming multiprotein complexes that, through modification of chromatin structure, repress target gene expression (Fig. 4). Three potential E2F regulated PcG genes, Enhancer of Zeste Homolog 2 (EZH2), Embryonic Ectoderm Development (EED), and Suppressor of Zeste 12 (SUZ12), constitute the Polycomb repressive complex 2 (PRC2) [78, 79] and it requires an intact SET domain (for methylation of histone tails) and endogenous histone deacetylase activity for its function [80, 81]. EZH2 and EED are also essential for the proliferation of both transformed and non-transformed cells and are under the regulation of the pRB-E2F pathway. EZH2 overexpression is associated with poor prognosis in patients with metastatic disease [78–80]. EZH2 promotes a reduction in the pool of insoluble F-actin and regulates cell adhesion and migration in invasive CaP cells [82, 83] and may control gene function via regulation of nuclear actin that is associated with the chromatin remodeling complex. Su et al. [84] demonstrated the existence of a cytosolic EZH2-containing methyltransferase complex that controls cellular signaling via ligand induced actin polymerization. Pharmacologic interference of EZH2 function selectively induces apoptosis in cancer, but not in normal cells and accessibility is dictated broadly by the degree of chromatin compaction, which is influenced in part by polycomb group proteins [85]. PRC2 catalyzes trimethylation of histone H3 lysine 27 (H3K27me3) [86]. H3K27me3 may also recruit DNA methyltransferases, and histone deacetylases, resulting in additional transcriptional repressive marks and heterochromatin compaction. Hence, overexpression of EZH2 is a marker of advanced and metastatic disease in many solid tumors, including prostate and breast cancer [86].

As another related clinically translational event, Laitinen et al. [87] suggested that demonstration by IHC of low Ki-67 (0–1 %) (a measure of cell proliferation) and EZH2 (<50 %) identifies a subgroup of patients with a very low risk of CaP, and could be candidates for active surveillance instead of immediate prostatectomy. Jhavar et al. [88] showed that Ki-67 expression is an independent determinant of very high risk among men enrolled in an active surveillance cohort. Hence, the degrees of expression of EZH2 combined with a measure of cell proliferation are potential prognostic biomarkers of the severity of CaP and other solid tumors.

Because our group has characterized the clinical relevance of nuclear features that can predict biochemical recurrence, metastasis, and CaP-specific survival we also have been studying what molecular mechanisms may cause such changes [7, 9, 24–29, 89]. The literature supports that changes in nuclear morphology are associated with deregulation of nuclear matrix proteins [50, 63] and abnormal expression of lamins [45, 47–49] and PcG [76, 90] genes and such changes have been found in undifferentiated neoplastic cells. Nuclear size and shape factors, especially mean nuclear area, have been shown to correlate with the Gleason score tissue architecture [91]. Debes et al. [92] demonstrated that the p300 histone acetyltransferase (HAT), a transcriptional regulator, is overexpressed in CaP and correlates specifically to nuclear

alterations in terms of DNA content, size, and shape. These nuclear alterations were seen in prostate biopsies and in CaP cell lines transfected with p300. Subsequently, Isharwal et al. [24] confirmed that p300 protein expression measured by IHC significantly correlated with nuclear alterations seen in tumor cells; specifically with DNA content ($p=0.016$), circular form factor ($p=0.012$) and minimum feret ($p=0.048$). Nuclear size and shape factors, especially mean nuclear area, were concordant with the Gleason score. Activation of the PcG proteins through p300 and perhaps EZH2 may regulate, in part, nuclear size and shape via the histone modifications and may provide a tool for evaluation of the pathological status of CaP [93]. Recently, Imbalzano et al. [94] have demonstrated that the SWI/SNF chromatin remodeling enzyme ATPase and the Brahma-related gene 1 (BRG1) contributes to the regulation of overall nuclear size and shape of immortalized mammary epithelial cells. Notably, they observed in BRG1 knockdown cells the formation of grooves at the nuclear periphery; however, there were no changes in levels of the nuclear structure markers lamin A/C, lamin B, emerin, nesprin, nurim, and the splicing speckle component SRm160. In addition, no changes in immunostaining for H1 or the modified histones phospho-H3Ser10 and H3triMeK4 were observed. This recent finding suggests that BRG1 can also mediate cancer nuclear shape by internal nuclear mechanisms that likely control chromatin dynamics. Hence, BRG1, p300, and other epigenetic histone-mediated processes of the PcG complexes noted above can alter nuclear structure in cancer.

Another central aspect of nuclear architecture is the nuclear matrix [95–97], which is composed in large part of the ribonucleoprotein (RNP) network, packaged amongst a multitude of proteins (<400) that form a non-chromatin structure throughout the nucleoplasm. Infrequent and specific matrix attachment regions (MARs) and scaffold-associated regions (SARs) of chromatin fibers bind the nucleoskeleton and support the chromatin loop domains and high mobility group nucleosome-non-histone binding (HMGN) [98] proteins that play an intricate role in chromatin structure and function [46, 50, 91]. The nuclear matrix also interconnects with the nuclear lamina (a fibrous meshwork of intermediate filament lamins and associated proteins underlying the inner nuclear membrane) and intranuclear lamin subassemblies, which interact with chromatin [35, 38, 39, 41, 44, 97]. Since the nuclear lamins are attached directly to NETs in the inner nuclear membrane and are bound to the heterochromatin structure, they provide a scaffold for organization of numerous nuclear functions tied to a variety of proteins [45, 46, 98–101]. The nuclear lamins have roles in epigenetics, chromatin organization, DNA replication, transcription, and DNA repair, normal cellular aging, stem cell renewal, virus infections, and cancer [101]. Mutations in the lamin genes are linked to a variety of degenerative laminopathies, whereas changes in the expression of lamins are associated with tumorigenesis and also telomere structure, length, and function, and in the stabilization of the DNA damage repair response pathway [102]. The NE and its NET proteins are involved in maintaining and/or disrupting chromatin organization and nuclear architecture during cell division, human embryonic stem cell differentiation, and tumorigenesis dedifferentiation, and therefore, understanding these processes has potential clinical translational value [53, 65, 95–104].

Lamins play key roles in preserving several genome functions (e.g., higher-order genome organization and stability, chromatin regulation, transcription, DNA replication, and maintenance of telomeres) [45–48, 95–104] as well as being critical for maintaining nuclear architecture [95–97]. The importance of the NE and the lamins are well known in tumor development and progression [35]. Lamins are associated with proliferation and cell motility and they can serve as prognostic biomarkers in solid tumors [104]. Coradeghini et al. demonstrated differential expression of lamins A/C and B in CaP, with lamin B expression correlating with increasing Gleason grade [105]. Skvortsov et al. [106] showed that lamin-A/C expression correlated with the different Gleason groups. Compared to paired benign samples, lower Gleason score tumors showed down-regulation of lamin A/C in 60 % of CaP cases while higher Gleason score tumors revealed upregulation in 70 % of cases. To confirm lamin A/C regulation the authors used IHC to successfully confirm the differences between benign tissue, lower and higher Gleason score tumors using tissue microarrays of an independent set of some 90 tumor cases (ROC AUC = 0.88). Kong et al. [107] demonstrated that lamin A/C is overexpressed in invasive CaP. Their data showed that lamin A/C proteins are positively involved in malignant behavior of CaP cells in vitro and confirmed their data using IHC with a tissue microarray made up of 376 tissue cores of 94 CaP cases. Also, their data support that the mechanism goes through the PI3K/AKT/PTEN pathway and lamin A/C may represent a new and a novel therapeutic target for CaP. Though the lamins appear to be closely involved in the tumor biology events such as motility, proliferation, and invasiveness; their role in altering nuclear morphology occasionally has become controversial [94, 108, 109].

## Conclusions

In summary, the nuclear envelope and its numerous associated proteins (lamins A/C and B, emerin, LAP2, BRG1, nesprin 1 and 2, the nucleoporins NUP88, 98, 133, 214, etc.) and key nuclear structural elements (i.e., nuclear matrix, actin, and lamins) play significant roles in chromatin spatial organization. Additionally, these elements maintain internal nuclear architecture, genome stability, and normal cellular processes (e.g., DNA repair, signaling, cell cycle, and mitosis). The human cell has evolved into a highly ordered biological machine driven by energy and the need to sustain spatial geometry of DNA and chromatin and the protein-related functions associated with maintenance of the nuclear apparatus. However, in disease this well-engineered cellular machine fails and often the built-in repair mechanisms also fail or may in fact accelerate the disease (e.g., autoimmune and malignant disease). Given all that we have discussed; where are the best molecular pathways or targets in either the primary cancer biopsy specimen or a benign area that identifies a lethal cancer and does so early? In both androgen-dependent and -independent CaP, we have noted the importance of critical targets including the PcG, enzyme-driven histone modifications, lamins A/C and B, BRG1, and p300. Also, there exists strong

evidence that the environment (androgens, infection, diet, metabolism, temperature, etc.) can produce several genetic and epigenetic changes that disrupt normal cellular functions related to nuclear architecture, genome stability, DNA repair mechanisms, and some have been noted above [52, 53, 55, 56, 58]. One certainty is that nuclear morphology is often disrupted early in cancer with respect to nuclear size, shape, DNA content (ploidy), and chromatin organization. Does the entire target organ possess molecular and/or structural changes (field effects) that may differentiate a lethal and nonlethal cancer? Given the importance of nuclear shape to prognosis of cancer phenotypes, it is surprising and frustrating that we currently lack a detailed understanding to explain these changes and how they might arise and relate to specific molecular pathways in the cancer cell. This review offers an attempt to explain parts of this dilemma, at least in CaP. Finally, what are some of the NETs and their multiple attachments (at the periphery and internally) to chromatin, DNA, telomeres, etc. Additionally, how do these interactions play a role in modification of nuclear morphometry, chromosome organization, and molecular regulatory events that are clinically more useful in early prognosis and identifying new potential therapeutic targets of hormone-dependent and independent tumors?

# References

1. Virchow R (1863) Cellular pathology as based upon physiological and pathological histology. J B Lippincott, Philadelphia, PA
2. Beale L (1860) Examination of sputum from a case of cancer of the pharynx and the adjacent parts. Arch Med (Lond) 2:44–46
3. Long SR, Cohen MB (1993) Classics in cytology. VI: the early cytologic discoveries of Lionel S. Beale. Diagn Cytopathol 9(5):595–598
4. Cremer T, Cremer C (2006) Rise, fall and resurrection of chromosome territories: a historical perspective. Part II. Fall and resurrection of chromosome territories during the 1950s to 1980s. Part III. Chromosome territories and the functional nuclear architecture: experiments and models from the 1990s to the present. Eur J Histochem 50(4):223–272
5. Cremer T, Cremer C (2006) Rise, fall and resurrection of chromosome territories: a historical perspective. Part I. The rise of chromosome territories. Eur J Histochem 50(3):161–176
6. Boveri T (2008) Concerning the origin of malignant tumours by Theodor Boveri. Translated and annotated by Henry Harris. J Cell Sci 121(Suppl 1):1–84
7. Veltri RW, Christudass CS, Isharwal S (2012) Nuclear morphometry, nucleomics and prostate cancer progression. Asian J Androl 14(3):375–384
8. Cremer T, Cremer M (2010) Chromosome territories. Cold Spring Harb Perspect Biol 2(3):a003889
9. Veltri RW, Partin AW, Miller CM (2005) Quantitative nuclear grade (QNG): the clinical applications of the quantitative measurement of nuclear structure using image analysis. In: Kelloff GJ, Hawk ET, Sigman CC (eds) Cancer chemoprevention. Humana Press, Totowa, NJ, pp 97–108
10. Sheehan DC, Hrapchak BB (1980) Theory and practice of histotechnology, 2nd edn. Battelle, Columbus, OH
11. Papanicolaou GN, Traut HF (1997) The diagnostic value of vaginal smears in carcinoma of the uterus. 1941. Arch Pathol Lab Med 121(3):211–224
12. Gill JE, Jotz MM (1976) Further observations on the chemistry of pararosaniline-Feulgen staining. Histochemistry 46(2):147–160

13. Schulte E, Wittekind D (1989) Standardization of the Feulgen-Schiff technique. Staining characteristics of pure fuchsin dyes; a cytophotometric investigation. Histochemistry 91(4):321–331
14. Gleason DF (1966) Classification of prostatic carcinomas. Cancer Chemother Rep 50(3):125–128
15. Gleason DF (1992) Histologic grading of prostate cancer: a perspective. Hum Pathol 23(3):273–279
16. Epstein JI (2010) An update of the Gleason grading system. J Urol 183(2):433–440
17. Brimo F et al (2013) Contemporary grading for prostate cancer: implications for patient care. Eur Urol 63(5):892–901
18. Diamond DA et al (1982) Computerized image analysis of nuclear shape as a prognostic factor for prostatic cancer. Prostate 3(4):321–332
19. Benson MC, McDougal DC, Coffey DS (1984) The application of perpendicular and forward light scatter to assess nuclear and cellular morphology. Cytometry 5(5):515–522
20. Benson MC, McDougal DC, Coffey DS (1984) The use of multiparameter flow cytometry to assess tumor cell heterogeneity and grade prostate cancer. Prostate 5(1):27–45
21. Mohler JL et al (1988) Nuclear roundness factor measurement for assessment of prognosis of patients with prostatic carcinoma. II. Standardization of methodology for histologic sections. J Urol 139(5):1085–1090
22. Mohler JL et al (1988) Nuclear roundness factor measurement for assessment of prognosis of patients with prostatic carcinoma. I. Testing of a digitization system. J Urol 139(5): 1080–1084
23. Partin AW et al (1989) A comparison of nuclear morphometry and Gleason grade as a predictor of prognosis in stage A2 prostate cancer: a critical analysis. J Urol 142(5):1254–1258
24. Isharwal S et al (2008) p300 (histone acetyltransferase) biomarker predicts prostate cancer biochemical recurrence and correlates with changes in epithelia nuclear size and shape. Prostate 68(10):1097–1104
25. Badalament RA et al (1996) An algorithm for predicting nonorgan confined prostate cancer using the results obtained from sextant core biopsies with prostate specific antigen level. J Urol 156(4):1375–1380
26. Veltri RW et al (2002) Prediction of pathological stage in patients with clinical stage T1c prostate cancer: the new challenge. J Urol 168(1):100–104
27. Veltri RW et al (1996) Ability to predict biochemical progression using Gleason score and a computer-generated quantitative nuclear grade derived from cancer cell nuclei. Urology 48(5):685–691
28. Khan MA et al (2003) Quantitative alterations in nuclear structure predict prostate carcinoma distant metastasis and death in men with biochemical recurrence after radical prostatectomy. Cancer 98(12):2583–2591
29. Veltri RW et al (2004) Ability to predict metastasis based on pathology findings and alterations in nuclear structure of normal-appearing and cancer peripheral zone epithelium in the prostate. Clin Cancer Res 10(10):3465–3473
30. Kortenhorst MS et al (2009) Valproic acid causes dose- and time-dependent changes in nuclear structure in prostate cancer cells in vitro and in vivo. Mol Cancer Ther 8(4):802–808
31. Doyle S et al (2010) A boosted Bayesian multiresolution classifier for prostate cancer detection from digitized needle biopsies. IEEE Trans Biomed Eng 59(5):1205–1218
32. Madabhushi A et al (2011) Computer-aided prognosis: predicting patient and disease outcome via quantitative fusion of multi-scale, multi-modal data. Comput Med Imaging Graph 35(7–8):506–514
33. Gao M, Bridgman P, Kumar S (2003) Computer aided prostate cancer diagnosis using image enhancement and JPEG2000. In: Proceedings of the SPIE Annual Meeting, 2003, San Diego, CA
34. Tiwari P et al (2011) Multi-modal data fusion schemes for integrated classification of imaging and non-imaging biomedical data. In: ISBI, 2011, Chicago, IL, pp 165–168

35. Ali S et al (2011) Adaptive energy selective active contour with shape priors for nuclear segmentation and Gleason grading of prostate cancer. Med Image Comput Comput Assist Interv 14(Pt 1):661–669

36. Doyle S et al (2007) Automated grading of prostate cancer using architectural and textural image features. In: ISBI, 2007, Arlington, VA, pp 1284–1287

37. Huang PW, Lee CH (2009) Automatic classification for pathological prostate images based on fractal analysis. IEEE Trans Med Imaging 28(7):1037–1050

38. Khurd P et al (2010) Computer-aided Gleason grading of prostate cancer histopathological images using texton forests. In: ISBI, 2010, Rotterdam, pp 636–639

39. Khurd P et al (2011) Network cycle features: application to computer-aided Gleason grading of prostate cancer histopathological images. In: ISBI, 2011, Chicago, IL, pp 1632–1636

40. Naik S et al (2008) Automated gland and nuclei segmentation for grading of prostate and breast cancer histopathology. In: ISBI, Paris, 2008, pp 284–287

41. Nguyen K, Jain AK, Allen RL (2010) Automated gland segmentation and classification for gleason grading of prostate tissue images. In: 20th international conference on pattern recognition (ICPR), 2010, Istanbul, pp 1497–1500

42. Ou Y et al (2009) Sampling the spatial patterns of cancer: optimized biopsy procedures for estimating prostate cancer volume and Gleason Score. Med Image Anal 13(4):609–620

43. Tabesh A et al (2007) Multifeature prostate cancer diagnosis and Gleason grading of histological images. IEEE Trans Med Imaging 26(10):1366–1378

44. Yoon HY et al (2011) Cardinal multiridgelet-based prostate cancer histological image classification for Gleason grading. In: BIBM, 2011, Atlanta, GA, pp 315–320

45. Chow KH, Factor RE, Ullman KS (2012) The nuclear envelope environment and its cancer connections. Nat Rev Cancer 12(3):196–209

46. de Las Heras JI, Batrakou DG, Schirmer EC (2013) Cancer biology and the nuclear envelope: a convoluted relationship. Semin Cancer Biol 23(2):125–137

47. Verstraeten VL et al (2007) The nuclear envelope, a key structure in cellular integrity and gene expression. Curr Med Chem 14(11):1231–1248

48. Hozák P et al (1995) Lamin proteins form an internal nucleoskeleton as well as a peripheral lamina in human cells. J Cell Sci 108(Pt 2):635–644

49. Naetar N, Foisner R (2009) Lamin complexes in the nuclear interior control progenitor cell proliferation and tissue homeostasis. Cell Cycle 8(10):1488–1493

50. Berezney R, Coffey DS (1974) Identification of a nuclear protein matrix. Biochem Biophys Res Commun 60(4):1410–1417

51. Coffey DS (2002) Nuclear matrix proteins as proteomic markers of preneoplastic and cancer lesions: commentary re: G. Brunagel et al., nuclear matrix protein alterations associated with colon cancer metastasis to the liver. Clin. Cancer Res., 8: 3039–3045, 2002. Clin Cancer Res 8(10):3031–3033

52. Getzenberg RH, Coffey DS (2011) Changing the energy habitat of the cancer cell in order to impact therapeutic resistance. Mol Pharm 8(6):2089–2093

53. Hanahan D, Weinberg RA (2011) Hallmarks of cancer: the next generation. Cell 144(5):646–674

54. He S et al (2008) Chromatin organization and nuclear microenvironments in cancer cells. J Cell Biochem 104(6):2004–2015

55. Podlaha O et al (2012) Evolution of the cancer genome. Trends Genet 28(4):155–163

56. Schetter AJ, Heegaard NH, Harris CC (2010) Inflammation and cancer: interweaving microRNA, free radical, cytokine and p53 pathways. Carcinogenesis 31(1):37–49

57. Strahl BD, Allis CD (2000) The language of covalent histone modifications. Nature 403(6765):41–45

58. Turner BM (2011) Environmental sensing by chromatin: an epigenetic contribution to evolutionary change. FEBS Lett 585(13):2032–2040

59. Wu JI, Lessard J, Crabtree GR (2009) Understanding the words of chromatin regulation. Cell 136(2):200–206

60. Zhang Y, Reinberg D (2001) Transcription regulation by histone methylation: interplay between different covalent modifications of the core histone tails. Genes Dev 15(18): 2343–2360

61. Sasaki M et al (2002) Methylation and inactivation of estrogen, progesterone, and androgen receptors in prostate cancer. J Natl Cancer Inst 94(5):384–390

62. Suzuki H, Ito H (1999) Role of androgen receptor in prostate cancer. Asian J Androl 1(3):81–85

63. Tropberger P et al (2013) Regulation of transcription through acetylation of H3K122 on the lateral surface of the histone octamer. Cell 152(4):859–872

64. Jones PA, Baylin SB (2002) The fundamental role of epigenetic events in cancer. Nat Rev Genet 3(6):415–428

65. Cai C et al (2011) Androgen receptor gene expression in prostate cancer is directly suppressed by the androgen receptor through recruitment of lysine-specific demethylase 1. Cancer Cell 20(4):457–471

66. Chlenski A et al (2001) Androgen receptor expression in androgen-independent prostate cancer cell lines. Prostate 47(1):66–75

67. Aryee MJ et al (2013) DNA methylation alterations exhibit intraindividual stability and inter-individual heterogeneity in prostate cancer metastases. Sci Transl Med 5(169):169ra10

68. Jarrard DF et al (1998) Methylation of the androgen receptor promoter CpG island is associated with loss of androgen receptor expression in prostate cancer cells. Cancer Res 58(23):5310–5314

69. Izbicka E et al (1999) 5,6 Dihydro-5′-azacytidine (DHAC) restores androgen responsiveness in androgen-insensitive prostate cancer cells. Anticancer Res 19(2A):1285–1291

70. Seligson DB et al (2005) Global histone modification patterns predict risk of prostate cancer recurrence. Nature 435(7046):1262–1266

71. Bianco-Miotto T et al (2010) Global levels of specific histone modifications and an epigenetic gene signature predict prostate cancer progression and development. Cancer Epidemiol Biomarkers Prev 19(10):2611–2622

72. Watson JA et al (2010) Hyperacetylation in prostate cancer induces cell cycle aberrations, chromatin reorganization and altered gene expression profiles. J Cell Mol Med 14(6B): 1668–1682

73. Malik G et al (2007) SELDI protein profiling of dunning R-3327 derived cell lines: identification of molecular markers of prostate cancer progression. Prostate 67(14):1565–1575

74. Huisman A et al (2007) Discrimination between benign and malignant prostate tissue using chromatin texture analysis in 3-D by confocal laser scanning microscopy. Prostate 67(3):248–254

75. Li LC, Carroll PR, Dahiya R (2005) Epigenetic changes in prostate cancer: implication for diagnosis and treatment. J Natl Cancer Inst 97(2):103–115

76. Brock HW, van Lohuizen M (2001) The Polycomb group–no longer an exclusive club? Curr Opin Genet Dev 11(2):175–181

77. Jacobs JJ, van Lohuizen M (2002) Polycomb repression: from cellular memory to cellular proliferation and cancer. Biochim Biophys Acta 1602(2):151–161

78. Czermin B et al (2002) Drosophila enhancer of Zeste/ESC complexes have a histone H3 methyltransferase activity that marks chromosomal Polycomb sites. Cell 111(2):185–196

79. Varambally S et al (2002) The polycomb group protein EZH2 is involved in progression of prostate cancer. Nature 419(6907):624–629

80. van der Vlag J, Otte AP (1999) Transcriptional repression mediated by the human polycomb-group protein EED involves histone deacetylation. Nat Genet 23(4):474–478

81. Yu J et al (2007) A polycomb repression signature in metastatic prostate cancer predicts cancer outcome. Cancer Res 67(22):10657–10663

82. Bryant RJ et al (2008) The Polycomb Group protein EZH2 regulates actin polymerization in human prostate cancer cells. Prostate 68(3):255–263

83. Bettinger BT, Gilbert DM, Amberg DC (2004) Actin up in the nucleus. Nat Rev Mol Cell Biol 5(5):410–415

84. Su IH et al (2005) Polycomb group protein ezh2 controls actin polymerization and cell signaling. Cell 121(3):425–436

85. Tan J et al (2007) Pharmacologic disruption of Polycomb-repressive complex 2-mediated gene repression selectively induces apoptosis in cancer cells. Genes Dev 21(9):1050–1063

86. Chase A, Cross NC (2011) Aberrations of EZH2 in cancer. Clin Cancer Res 17(9):2613–2618

87. Laitinen S et al (2008) EZH2, Ki-67 and MCM7 are prognostic markers in prostatectomy treated patients. Int J Cancer 122(3):595–602

88. Jhavar S et al (2009) Biopsy tissue microarray study of Ki-67 expression in untreated, localized prostate cancer managed by active surveillance. Prostate Cancer Prostatic Dis 12(2):143–147

89. Veltri RW et al (2010) Nuclear roundness variance predicts prostate cancer progression, metastasis, and death: a prospective evaluation with up to 25 years of follow-up after radical prostatectomy. Prostate 70(12):1333–1339

90. Cao R et al (2002) Role of histone H3 lysine 27 methylation in Polycomb-group silencing. Science 298(5595):1039–1043

91. Bektas S et al (2009) The relation between Gleason score, and nuclear size and shape factors in prostatic adenocarcinoma. Turk J Med Sci 39(3):381–387

92. Debes JD et al (2005) p300 modulates nuclear morphology in prostate cancer. Cancer Res 65(3):708–712

93. Wang Z et al (2008) Combinatorial patterns of histone acetylations and methylations in the human genome. Nat Genet 40(7):897–903

94. Imbalzano KM et al (2013) Nuclear shape changes are induced by knockdown of the SWI/SNF ATPase BRG1 and are independent of cytoskeletal connections. PLoS One 8(2):e55628

95. Chernov IP, Akopov SB, Nikolaev LG (2004) Structure and functions of nuclear matrix associated regions (S/MARs). Russ J Bioorg Chem 30(1):1–11

96. Elcock LS, Bridger JM (2008) Exploring the effects of a dysfunctional nuclear matrix. Biochem Soc Trans 36(Pt 6):1378–1383

97. Nickerson J (2001) Experimental observations of a nuclear matrix. J Cell Sci 114(Pt 3):463–474

98. Postnikov Y, Bustin M (2010) Regulation of chromatin structure and function by HMGN proteins. Biochim Biophys Acta 1799(1–2):62–68

99. Dechat T et al (2008) Nuclear lamins: major factors in the structural organization and function of the nucleus and chromatin. Genes Dev 22(7):832–853

100. Prokocimer M et al (2009) Nuclear lamins: key regulators of nuclear structure and activities. J Cell Mol Med 13(6):1059–1085

101. Stuurman N, Heins S, Aebi U (1998) Nuclear lamins: their structure, assembly, and interactions. J Struct Biol 122(1–2):42–66

102. Gonzalez-Suarez I et al (2009) Novel roles for A-type lamins in telomere biology and the DNA damage response pathway. EMBO J 28(16):2414–2427

103. Butler JT et al (2009) Changing nuclear landscape and unique PML structures during early epigenetic transitions of human embryonic stem cells. J Cell Biochem 107(4):609–621

104. Goldman RD et al (2002) Nuclear lamins: building blocks of nuclear architecture. Genes Dev 16(5):533–547

105. Coradeghini R et al (2006) Differential expression of nuclear lamins in normal and cancerous prostate tissues. Oncol Rep 15(3):609–613

106. Skvortsov S et al (2011) Proteomics profiling of microdissected low- and high-grade prostate tumors identifies Lamin A as a discriminatory biomarker. J Proteome Res 10(1):259–268

107. Kong L et al (2012) Lamin A/C protein is overexpressed in tissue-invading prostate cancer and promotes prostate cancer cell growth, migration and invasion through the PI3K/AKT/PTEN pathway. Carcinogenesis 33(4):751–759

108. Foster CR et al (2010) Lamins as cancer biomarkers. Biochem Soc Trans 38(Pt 1):297–300

109. Reddy KL, Feinberg AP (2013) Higher order chromatin organization in cancer. Semin Cancer Biol 23(2):109–115